ISSN 2706-655X Vol.6, Issue 5: 41-46, DOI: 10.25236/IJFET.2024.060506

Research of highly birefringent photonic crystal fibers based on elliptical core arrays

Xuanjun He*

College of Physics and Optoelectronic Engineering, Shenzhen University, Shenzhen, 518000, China
**Corresponding author: hexuanjun9@gmail.com*

Abstract: *Photonic crystal fiber (PCF) is widely used in sensing applications due to its structural flexibility, high birefringence, low confinement loss, and significant nonlinear effects. This study presents a novel design of a highly birefringent photonic crystal fiber with a core filled with carbon disulfide (CS_2). The simple structure of the fiber improves its manufacturability and performance by optimizing the number and shape of elliptical pores in the core. Using the finite element method (FEM) combined with perfectly matched layer (PML) boundary conditions, the birefringence, mode field area, and confinement loss were analyzed at different wavelengths. The results indicate that the newly designed fiber significantly outperforms existing liquid-sensing photonic crystal fibers, especially in the near-infrared region, making it a promising candidate for high-sensitivity applications.*

Keywords: *Photonic Crystal Fiber, High Birefringence, Liquid Core*

1. Introduction

Photonic crystal fiber (PCF) has achieved a wide range of applications in the field of sensing due to its flexibility in structural design, high birefringence, low confinement loss, high sensitivity, flat dispersion characteristics and significant nonlinear effects [1,2]. Nowadays, PCF has been widely used in many fields such as temperature sensing [3,4], biological sensing, chemical sensing [5] and optical communication [6] by filling the air holes with gases, liquids or metallic materials, which fully demonstrates its great practical value and application prospect.

Birefringence is a unique optical property of optical fibers that can significantly improve the sensitivity of fiber optic sensors by enhancing the interaction between light and the target analyte[7]. Therefore, the development of fiber optic sensors with high birefringence properties is not only of great significance in the field of scientific research, but also shows great promise and potential in practical applications.

In recent years, researchers have begun to focus on improving the birefringence and sensitivity of optical fibers by introducing various analytes into the fiber core or cladding. Although several PCF structures have been proposed and these designs have made significant progress in birefringence and sensitivity, most of them are complex, difficult to fabricate, and have low sensitivity at 1.3 μm wavelength. To solve these problems and achieve high sensitivity and high birefringence for liquid sensing, this study presents a novel PCF design in which the core material is carbon disulfide (CS_2). The PCF has a simple structure, is easy to fabricate, and improves performance by optimizing the number and shape of elliptical pores in the core. Numerical simulations of this fiber were carried out using the finite element method combined with perfectly matched layer boundary conditions to analyze its birefringence, mode-field area, and confinement loss characteristics in different wavelength ranges. The results show that the newly designed fiber shows a significant improvement in performance compared to existing liquid sensing PCFs.

2. Theoretical Models

2.1 Finite Element Method

Finite Element Method (FEM) is a numerical analysis technique widely used to simulate and analyze the electromagnetic field distribution of complex structures. In the study of PCFs, the full vector FEM combined with perfect boundary conditions is used to accurately simulate and analyze the mode fields

ISSN 2706-655X Vol.6, Issue 5: 41-46, DOI: 10.25236/IJFET.2024.060506

of optical fibers [8]. The method divides the mode field of the fiber into fine grid cells, each with close dimensions, ensuring the accuracy and reliability of the analysis.

In the simulation process, mathematical-physical models are first developed for each mesh, and approximate equations for analyzing the modes in the frequency domain are constructed based on different discretized models. The waveguide equations are $n(\nabla E) - jk(En) = 0$ and form the stiffness matrix [9]. By combining Maxwell's equations, the initial equation is:

$$\nabla \times \left(\left| \mu_r \right|^{-1} \nabla \times \vec{E} \right) - \kappa_0^2 \varepsilon_r \vec{E} = 0, \tag{1}$$

where $\kappa_0 = 2\pi / \lambda$ is the wave number of the vacuum, ε_r and μ_r and are the relative permittivity and relative permeability of the medium, respectively.

In order to accurately simulate air-hole boundaries, the line-mixing boundaries or nodes are often selected as simulation tuples, and the fiber end face is divided into many tuples, and the eigenvalue equations of the tuples can be obtained by solving these tuples using Eq. (1):

$$[\kappa]\{\vec{E}\} = \kappa_0^2 n_{eff}^2 [M]\{\vec{E}\}, \tag{2}$$

where κ and M are finite element matrices. The eigenvalue equations are solved based on the sparse matrix properties of κ and M to obtain the PCF and the fundamental mode effective refractive index n_{eff}.

2.2 Birefringence

The birefringence coefficient B is calculated from the difference between the effective refractive indices in the polarization directions of the two polarizations of x and y. The birefringence coefficient describes the bias-preserving property of an optical fiber where, due to the strong birefringence effect, the propagation constants of the two polarization modes are different and thus their relative phases become progressively larger. High birefringence indicates that the fiber is polarization-preserving. Therefore, the propagation of light waves in optical fibers is guaranteed to be unaffected by fiber bending and temperature. The coefficient of birefringence B is given by

$$B = \frac{\left| \beta_x - \beta_y \right|}{\kappa_0} = \frac{2\pi \left| \beta_x - \beta_y \right|}{\lambda} = \left| \mathrm{Re}\left(n_{eff}^x \right) - \mathrm{Re}\left(n_{eff}^y \right) \right|, \tag{3}$$

where B denotes the birefringence of the PCF, and n_{eff}^x and n_{eff}^y are the effective refractive indices for x- and y-polarization, respectively.

2.3 Effective Mode Field Area

A quantitative measure of the amount of transverse area occupied by a mode in a waveguide or fiber. In general, the larger the mode field area, the lower the nonlinearity coefficient for a given power, so large mode fields generally correspond to high power or light intensity. The effective mode field area has a key influence on the measurement of the nonlinearity coefficient. The effective mode field area A_{eff} formula is as follows [10]:

$$A_{eff} = \frac{\left| \iint \left| E^2 \right| dxdy \right|^2}{\iint \left| E \right|^4 dxdy}. \tag{4}$$

2.4 Confinement Loss

The larger its value, the transmission of optical signal power will be faster attenuation, the more unfavorable in the optical fiber remote sensing equipment. The formula for the limiting loss L (dB/km) is as follows:

ISSN 2706-655X Vol.6, Issue 5: 41-46, DOI: 10.25236/IJFET.2024.060506

$$L = \frac{20}{\ln 10}\frac{2\pi}{\lambda}\mathrm{Im}\left(n_{eff}\right)\times 10^{9}, \tag{5}$$

where λ (μm) is the wavelength of the light wave and $Im(n_{eff})$ is the imaginary part of the effective refractive index of the mode.

3. PCF Structure Design

3.1 Modeling and Structural Parameters

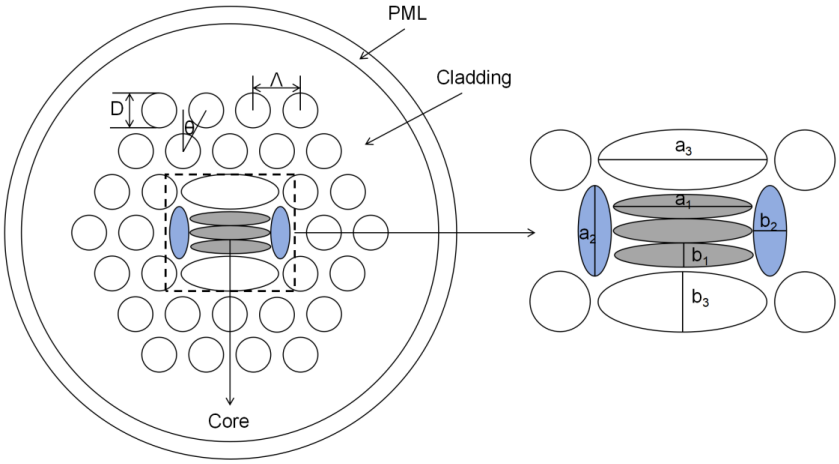

Figure 1: Schematic diagram of PCF structure

As shown in Fig. 1, this is a fiber structure design with a high degree of asymmetry. The cladding material is SiO_2 and a perfect match layer of 2.0 μm is added on the outside. The core is a tri-elliptic array and the material is CS_2, where the structural parameters are a_1 = 4.6 μm and b_1 = 0.8 μm. It is flanked by elliptical holes filled with C_2H_5OH with parameters a_2 = 3.0 μm and b_2 = 1.1 μm, respectively. The rest of the circular air holes are arranged similarly to the conventional PCF structure with a hexagonal array, where D = 2.0 μm, Λ= 2.7 μm, $\theta = \pi/6$. However, to further enhance the birefringence properties of this fiber, in this paper, the original four circular air holes on the top and bottom of the core are replaced by elliptical air holes with dimensions a_3 = 5.6 μm, b_3 = 2.0 μm. This makes the overall asymmetry more pronounced and further improves the bias-maintaining properties.

3.2 Material refractive index

The refractive index of all materials in the article is determined using the Sellmeier formula [11].

$$n^2(\lambda) = 1 + \sum_{i=1}^{k}\frac{A_i\lambda^2}{\lambda^2 - \lambda_i^2} \tag{6}$$

According to equation (7), the refractive index of the CS_2 is [12]:

$$n_{CS_2} = 1.580826 + 1.52389\times10^{-2}\lambda^{-2} + 4.8578\times10^{-4}\lambda^{-4} - 8.2863\times10^{-5}\lambda^{-6} + 1.4619\times10^{-5}\lambda^{-8} \tag{7}$$

The material used for the cladding is SiO_2. To achieve high birefringence properties, it is necessary to introduce asymmetry into the PCF, so the Sellmeier equation for the blue holes in Fig. 1 can be expressed in terms of the use of C_2H_5OH liquid [13]:

$$n_{C_2H_5OH}^2 = 1 + \frac{0.8318\lambda^2}{\lambda^2 - 0.0093} - \frac{0.1558\lambda^2}{\lambda^2 + 49.952} \tag{8}$$

ISSN 2706-655X Vol.6, Issue 5: 41-46, DOI: 10.25236/IJFET.2024.060506

4. Simulation Analysis

4.1 Birefringence Properties

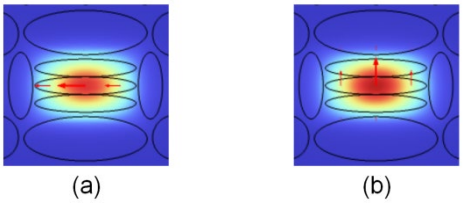

Figure 2: Cross section of the mode field distribution: (a) x-polarization (b) y-polarization

In this paper, a PCF structure based on a CS_2-filled core is proposed, and the mode field distributions of x-polarization and y-polarization at a wavelength of 1.55 μm are investigated. As shown in Fig. 2(a) and (b), the mode field distributions of the fundamental mode are effectively confined within the core region of the fiber, which fully demonstrates that the structure has a good confinement effect on the light waves, which is important for the transmission of light waves.

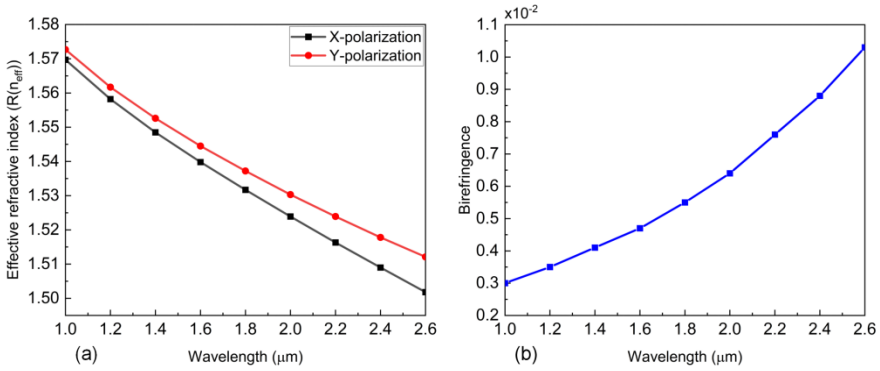

Figure 3: Refractive index studies: (a) variation of x and y polarization with wavelength (b) variation of birefringence with wavelength

The applicable wavelength range of this new fiber covers 1 to 3 μm, and the near-infrared wavelength band of 1-2.6 μm is investigated in this paper. As shown in Fig. 3, the effective refractive indices of x- and y-polarization decrease linearly with increasing wavelength, while the birefringence increase shows an increasing trend.

4.2 Transmission Characteristics

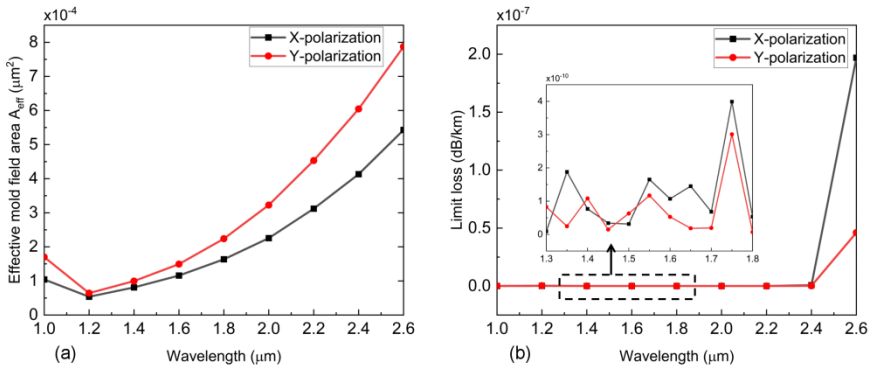

Figure 4: (a) Variation of effective mode field area with wavelength (b) Variation of limit loss with wavelength.

To analyze the transmission performance of this fiber, the effective mode field area and limiting loss were calculated using equations (4) and (5). Observing Fig. 4(a), the mode field area increases with increasing wavelength, except for a minimum at 1.2 μm. Figure 4(b), on the other hand, shows the loss, with the highest order of magnitude of the attenuation constant below 2.4 μm being 10^{-10}, while there is an increase of three orders of magnitude in the 2.6 μm and higher bands because the effect of confinement

ISSN 2706-655X Vol.6, Issue 5: 41-46, DOI: 10.25236/IJFET.2024.060506

will be reduced with the increase of wavelength. However, the confinement loss within the wavelength of 1-2.4 μm is rather low and in the magnitude of 10^{-10} which means that almost no mode energy will be wasted, although some tiny fluctuations can be observed. Further studies for the communication band show that the loss in the range of 1.3 to 1.8 μm is of very low order, indicating that the energy is well confined and little affected by the wavelength.

5. Exploration of Structural Parameters

5.1 Core Arrays and Air Hole Cycles

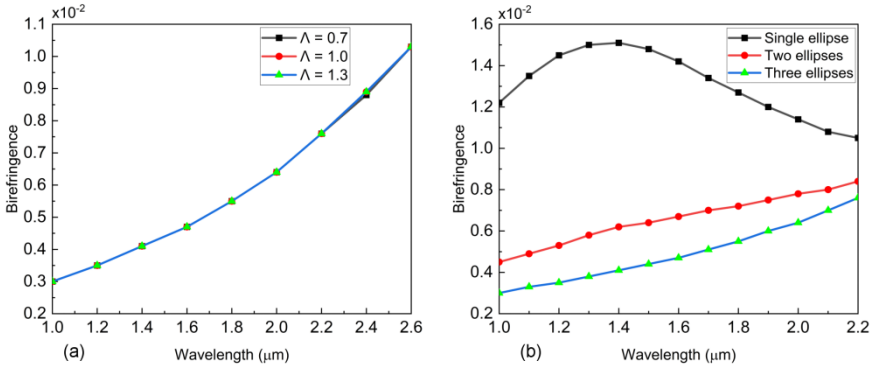

Figure 5: (a) Impact of cyclical variations (b) The effect of the number of ellipses

In this study, the cycle of air holes was first analyzed. The effects of periods of 0.7, 1.0, and 1.3 μm on the birefringence are shown in Fig. 5(a), and it can be observed that the three curves almost overlap, suggesting that the limiting capability of this fiber is mainly provided by the core, and the effect of the period of the air holes is weak.

Therefore, this paper makes adjustments to the fiber core array. As shown in Figure 5(b), only 1 to 2.2 μm are compared because reducing the number of ellipses compresses the applicable bands. It can be seen that the birefringence of a single ellipse, although the highest, has an undesirable linearity and trend. In contrast, double and triple ellipses have similar performance.

5.2 Ellipticity

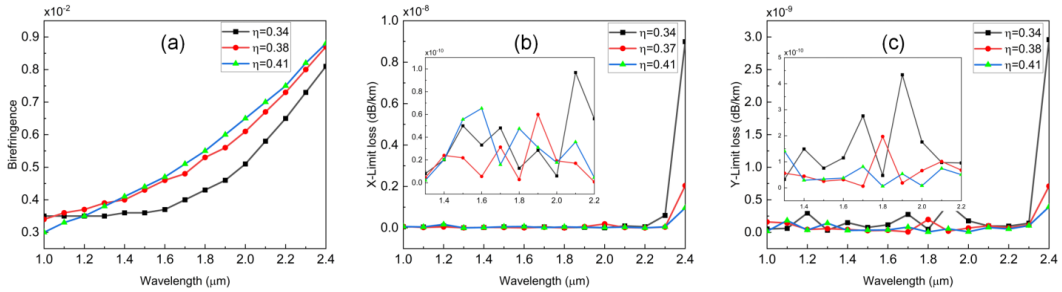

Figure 6: (a) Effect of ellipticity on birefringence (b) Effect of ellipticity on limiting loss (x-polarization) (c) Effect of ellipticity on limiting loss (y-polarization)

Synthesizing the birefringence performance and the applicable wavelength range, the tri-elliptic array is still used as the basic structure, and the ellipticity η = 0.34, 0.38, 0.41 is compared. As shown in Fig. 6(a), it is clear that the larger the ellipticity, the stronger the birefringence effect. While observing Fig. 6(b) and (c), the ellipticity effect is not significant in the communication band due to the small limiting loss, but considering longer wavelengths, a larger ellipticity has a stronger collection capability for optical signals.

6. Conclusions

This paper presents a novel photonic crystal fiber (PCF) with a carbon disulfide (CS_2) filled core, carefully designed to enhance both birefringence and sensitivity for liquid sensing applications. Using

ISSN 2706-655X Vol.6, Issue 5: 41-46, DOI: 10.25236/IJFET.2024.060506

the finite element method (FEM) and perfectly matched layer (PML) boundary conditions, the research simulated and analyzed the properties of this PCF, revealing significant performance improvements over existing designs. The effective mode field area, birefringence, and confinement loss were thoroughly evaluated, demonstrating the fiber's exceptional potential for practical application in various sensing environments.

These results indicate that the newly designed PCF not only simplifies structural complexity, but also significantly improves performance metrics, making it a promising candidate for high-sensitivity sensing technologies. The improved birefringence and reduced confinement loss are particularly beneficial for applications requiring precise and reliable measurements. This innovative design paves the way for further advancements in the development of high-performance PCFs, potentially changing the landscape of fiber-based sensing. Future work will focus on optimizing design parameters and exploring real-world applications to fully exploit the capabilities of this novel fiber.

References

[1] ZHAO Lijuan, ZHAO Haiying, XU Zhiniu. Design of high sensitivity static pressure sensor based on Brillouin dynamic grating [J]. Journal of Photonics, 2021,50(02):29-44.

[2] Md. Faizul Huq Arif, Md. Jaminul Haque Biddut. A new structure of photonic crystal fiber with high sensitivity, high nonlinearity, high birefringence and low confinement loss for liquid analyte sensing applications [J]. Sensing and Bio-Sensing Research, 2017, 12(4): 8-14.

[3] LIU X Y, BIN Y, Li H S, et al. Highly sensitive sensor for simultaneous underwater measurement of salinity and temperature based on highly birefringent asymmetric photonic crystal fiber [J]. Results in Optics, 2023, 11:100406

[4] HOSSAIN M S, MOHAMMAD F. Theoretical Investigation of Mid Infrared Temperature Sensor Based on Sagnac Interferometer Using Chloroform Filled Photonic Crystal Fiber[J] IEEE sensors journal, 2021,21(21):24157-24165

[5] SUDHIR K, DILIP K. Lower index liquid chemical detection by using photonic crystal fiber sensor [J]. Materials Today: Proceedings, 2022, 64(1): 69-73.

[6] VAN B C, HAI T T, THAO N T, et al. Experimental study of supercontinuum generation in water-filledcladding photonic crystal fiber in visible and near-infrared region [J]. Optical and Quantum Electronics, 2023, 3(55):1-14.

[7] LI Yizhou, TAN Fang, LIU Runze, et al. Performance study of highly birefringent elliptical core-like rectangular arrangement photonic crystal fiber[J]. Journal of Changchun University of Science and Technology (Natural Science Edition), 2024,47(02):23-30.

[8] BRECHET F, JACQUES M, DOMINIQUE P, et al. Complete analysis of the characteristics of propagation into photonic crystal fibers, by the finite element method[J]. Optical Fiber Technology, 2000, 6:181-191.

[9] Wang G, An L .COMSOL Multiphysics Engineering Practice and Theoretical Simulation [M]. Beijing: Electronic Industry Press, 2012.

[10] Wang Chengcheng, Zhang Feng, Wu Genzhu . Asymptotic terahertz porous photonic crystal fiber mode characterization [J]. Laser Technology, 2019, 43(6):768-772.

[11] LIU Tiecheng, HU Jingpei, ZHU Linglin, et al. Experimental study of Sellmeier model characterizing the birefringence dispersion of hybrid liquid crystals[J]. China Laser, 2020, 47(08):155-160.

[12] Zhang R, Giessen H. Theoretical design of a liquid-core photonic crystal fiber for supercontinuum generation [J]. Opt. Express, 2006, 14:6800-6812.

[13] Rasoul Raei, Majid Ebnali-Heidari, Hamed Saghaei. Supercontinuum generation in organic liquid-liquid core-cladding photonic crystal fiber in visible and near-infrared regions[J]. J. Opt. Soc. Am. B, 2018, 35:323-330.